PERGAMON

Journal of Structural Geology 24 (2002) 1829–1844

JOURNAL OF STRUCTURAL GEOLOGY

www.elsevier.com/locate/jstrugeo

H*T*-deformation of garnet: an EBSD study on granulites from Sri Lanka, India and the Ivrea Zone

R. Kleinschrodt[a,*], J.P. Duyster[b]

[a]*Institut für Mineralogie und Geochemie, Universität Köln, Zülpicher Str. 49b, D-50674 Köln, Germany*
[b]*Institut für Geologie, Mineralogie und Geophysik, Ruhr-Universität Bochum, Universitätsstr. 150, D-44780 Bochum, Germany*

Received 28 March 2001; revised 6 December 2001; accepted 10 December 2001

Abstract

Garnets from three regional granulite terrains (Sri Lanka, Eastern Ghats, Ivrea Zone) have been analyzed and the results indicate, that garnet can be plastically deformed by dominant dislocation glide/creep with variable dominant slip systems.

Garnets from a granulite facies fold hinge in a quartzite of the Highland Complex of Sri Lanka, unequivocally attest to plastic deformation of garnet. Outside the fold hinge the garnets form flat discs elongated parallel to a pronounced stretching lineation and show deformation microstructures like boudinage and pinch and swell structures. In the fold hinge these garnet discs are folded within the quartzitic matrix at temperatures of about 800 °C. In spite of the preservation of deformed shapes, intracrystalline deformation microstructures are scarce. The garnets have distinct crystallographic preferred orientations, which can be interpreted by a dominant 1/2⟨111⟩{110} slip system approaching 'easy slip' positions. These are reached rapidly under moderate strains as necessary lattice rotations are small.

Similar slip systems were derived for a garnet-bearing quartzite from the Eastern Ghats deformed at temperatures of 750–800 °C, but with more influence of initial orientation of garnets. Completely different textures indicative of dominant ⟨100⟩ [010] slip were found in a restitic garnet–sillimanite granulite from the Ivrea Zone. The variable deformation features and variable slip systems with 1/2⟨111⟩ and ⟨100⟩ Burgers vectors prove that garnets bear significant potential for contributing additional information on the H*T*-deformation of rocks.

Keywords: Garnet plasticity; Garnet microstructures; Deformation mechanisms; EBSD analysis; Granulites; Sri Lanka

1. Introduction

Since the development of electron channeling pattern analysis (ECP) and electron back scattered diffraction techniques (EBSD, OC-imaging) (for a review of the techniques see Lloyd (1987, 1994) and Prior et al. (1999)) the deformational behavior of garnet has received a lot of attention. Plastic deformation of garnet in nature is a matter of debate still, even though TEM work in recent years has documented that dislocations and dislocation networks form during experimental deformation of natural and synthetic garnets (Ji and Martignole, 1994; Karato et al., 1995; Voegele et al., 1998) suggesting dislocation glide or dislocation creep being active (Prior et al., 1999, 2000). Mechanisms different from crystal plasticity proposed to account for the elongate shape of garnet are fracture sliding, preferred growth, or solution/precipitation processes (e.g. Blackburn and Dennen, 1968; Dalziel and Bailey, 1968; den Brok and Kruhl, 1996). All of these mechanisms seem to be active under specific conditions and arguments for any one of these mechanisms are often ambiguous.

The presence of dislocations and subgrains was used as the main argument for crystal–plastic deformation being caused by dominant dislocation glide under high-grade conditions (Ji and Martignole, 1994), but OC-imaging of garnet microstructures (Prior et al., 1996) has revealed that even garnets from lower grade rocks (amphibolite to upper greenschist facies) with grain shapes not indicative of plastic deformation, have numerous dislocations or subgrains. So if dislocations and subgrains are found in elongate garnets, these are not necessarily linked to the high temperature part of the deformation path, a situation quite similar to that of quartz at lower temperatures. Kleinschrodt and McGrew (2000) showed that elongate garnets from a high strain zone in the granulites of Sri Lanka show a crystallographic preferred orientation (CPO) indicating dislocation glide with 1/2⟨111⟩{110} slip system being the dominant deformation mechanism.

* Corresponding author. Tel.: +49-221-470-3242; fax: +49-221-470-5199.

E-mail address: kleinsch@min.uni-koeln.de (R. Kleinschrodt).

0191-8141/02/$ - see front matter
PII: S0191-8141(01)00167-5

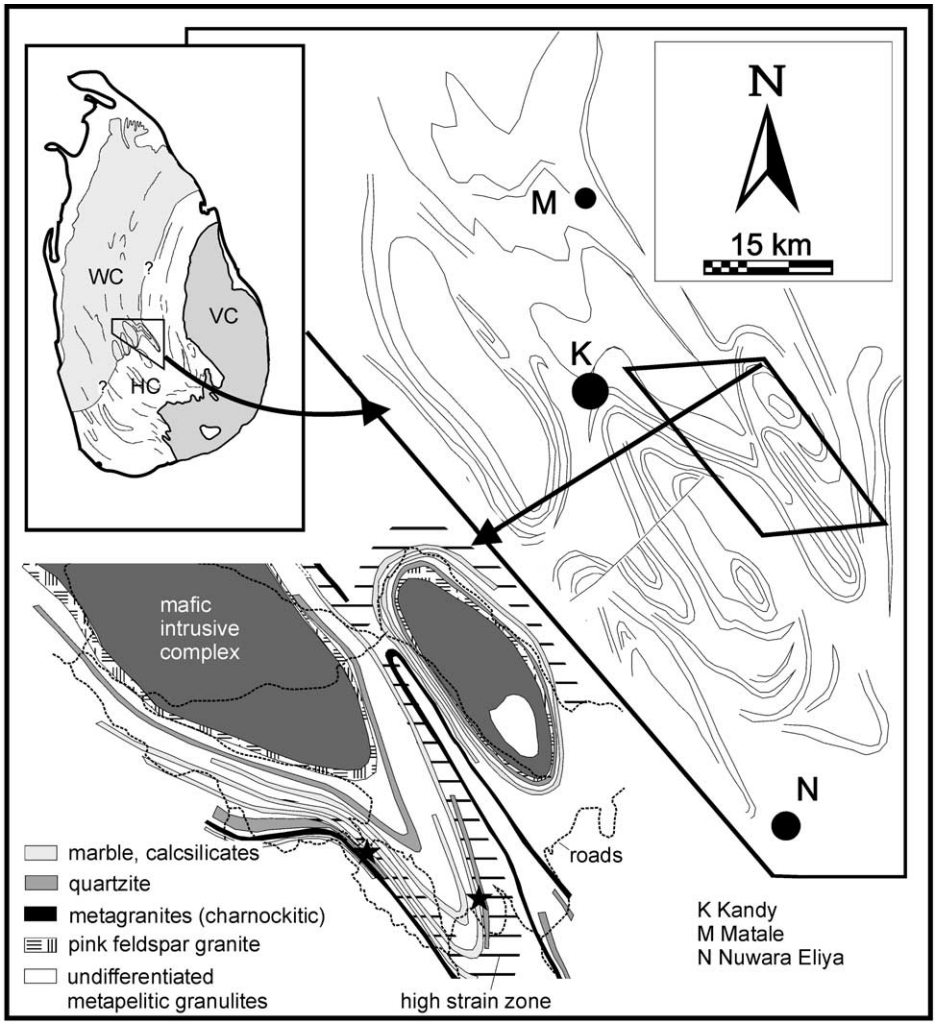

Fig. 1. Sample location of planar and folded garnet quarzite: about 15 km southeast of Kandy, within the Highland Complex, close to the southern hinge of the Dumbara Synform. The localities are marked with asterisks. Lines in the overview maps show general strike of prominent lithological contacts redrawn from the Geological map of Sri Lanka, 8 miles:1 inch (1982). WC Wanni Complex, HC Highland Complex, VC Vijayan Complex.

These garnets have low dislocation densities and are nearly free of subgrain structures, which would be expected in a dislocation dominated deformation regime. Therefore, again the question has to be raised whether the elongate shape and deformation microstructures like pinch and swell structures could not be explained by other processes.

In this study we investigate garnets from the Highland Complex of Sri Lanka which after stretching/flattening were deformed in a fold hinge. In this case all explanations not dealing with deformation by crystal plasticity which may be alternative explanations for the elongate shape and boudinage microstructures (e.g. preferred growth, 'spheroidization' of garnet fragments) can be ruled out. The development of the microstructures and textures of garnet in planar and folded quartzites was studied optically and with EBSD-techniques. Furthermore, garnet textures of granulite facies rocks from India (Eastern Ghats) and Italy (Ivrea Zone) are compared with the Sri Lankan examples.

2. Deformed garnet bearing rocks in Sri Lanka

Deformed garnets occur in quartzites in the high-grade Highland Complex of Sri Lanka. Conventional geothermobarometry in basic and metapelitic rocks interlayered with the quartzites yields peak temperatures of about 850 ± 50 °C at 9 ± 1 kbar (Kleinschrodt and Voll, 1994). The garnets have an almandine-rich composition (alm84 py14 sp2). Significantly elongated garnets occur in quartzites intercalated in a metapelitic sequence, both being deformed in a high-strain zone. This high-strain zone can be traced for several tens of kilometers in the surrounding of a large scale synform, the Dumbara Synform E of Kandy (Fig. 1) (Kleinschrodt and Voll, 1994). The high-strain zone formed after the peak of metamorphism, but at only slightly lower temperatures, still in the range of 750–800 °C (Voll et al., 1994). The fabrics of the high-strain zone are thoroughly equilibrated at high temperatures, so that intracrystalline deformation microstructures are scarce.

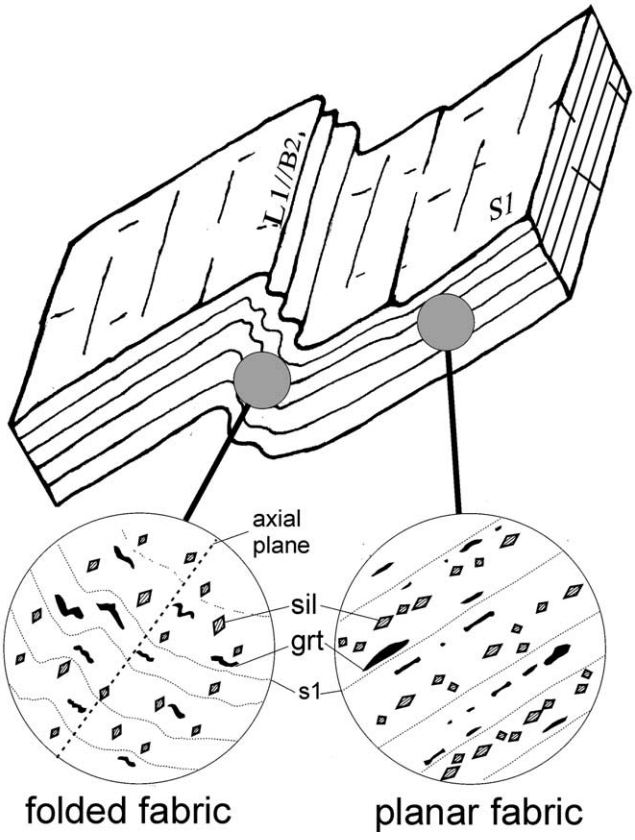

Fig. 2. Schematic block diagram of the position of planar and folded samples from limb and hinge area of a granulite–facies fold.

Monocline to isoclinal folds are found locally, folding the otherwise straight layering. The fold axis is parallel to the pronounced L1 stretching lineation. One such fold was found within the sequence of deformed metapelites, affecting also a garnet-bearing quartzite. A schematic sketch is shown in Fig. 2. Folding is only visible in quartzite samples, where thin feldspar layers mark S1 (S1, S2… according to Kleinschrodt and Voll (1994)). A crenulation of the feldspar-rich layers and a rough parting surface parallel to the axial plane mark S2 on the macroscopic scale but, generally, the axial plane cleavage is poorly developed since minerals defining such a plane, like sheet silicates or amphibole, are missing.

High-grade parageneses are stable during the formation of the large scale synform in the level of the high-strain zone and post-tectonic retrograde symplectitic breakdown of garnet to orthopyroxene and plagioclase in interlayered basic rocks, occurs at about 750–700 °C (Kleinschrodt and Voll, 1994).

3. Optical microstructures

The fabrics in the planar quartzites and granulites outside the fold hinge have already been described in detail (Kleinschrodt and McGrew, 2000). The essential features are summarized and contrasted with the microstructures in the fold hinge in the next section.

3.1. Planar fabrics

The dominant planar foliation (S1) is parallel to a compositional layering defined by quartzitic layers, layers of different feldspar content and sillimanite rich quartzitic layers. Garnets occur within all layers, but significantly elongate garnets are found only in the quartzitic layers, not in the feldspar rich ones. Quartz has coarsened to a grain size in the centimeter range in pure quartzites. Impurities like feldspar and, to a lesser extent, sillimanite and other accessory minerals (magnetite, ilmenite, zircon, rutile) pin the grain boundaries and restrict quartz coarsening. The quartz grains have highly irregular grain shapes and coarsely irregularly serrate boundaries, commonly pinned by secondary phases. Long axes of coarse quartz grains in *XZ* and *YZ* sections usually roughly follow the layering (*XZ* sections: Fig. 3a and b).

Feldspars are commonly enclosed by quartz and deformed to long streaks. They effectively inhibit grain growth in these plagioclase layers or lenses, i.e. feldspar grain-size is significantly lower compared with quartz in quartz-rich layers.

Sillimanite is perfectly oriented with its *c*-axis parallel to the stretching lineation (Fig. 3b). In *YZ*-sections a vague preferred orientation of (010), marked by the well developed cleavage plane of sillimanite, close to the foliation plane is visible.

Garnets occur as three distinct groups of grain size and shape in the quartzitic rocks:

- Large garnets in the milimeter- to centimeter-scale. They occur frequently with numerous inclusions of quartz and sometimes sillimanite. These larger garnets commonly are fragmented and can be found in different stages of drifting apart of the fragments. The fragments are slightly elongate and rotate with their flat faces towards the foliation plane by fracture sliding on suitable oriented planes (Fig. 3c).
- Numerous elongate garnets showing significant aspect ratios (2–12), pinch and swell structures and dumb-bell shapes (Fig. 3d and e).
- Very small garnets with low aspect ratios formed by pinching of the thickened ends of the dumb-bell shaped garnets and separating from the parent grain. In Fig. 3e several such fragments which all may be derived from the central grain are marked with arrows, at both sides of the central grain small parts are in the state of being pinched off. In *YZ*-sections aspect ratios are smaller and the pinch and swell type structures are rarely found. Usually the garnets are planar and well oriented with their intermediate axis parallel to the foliation.

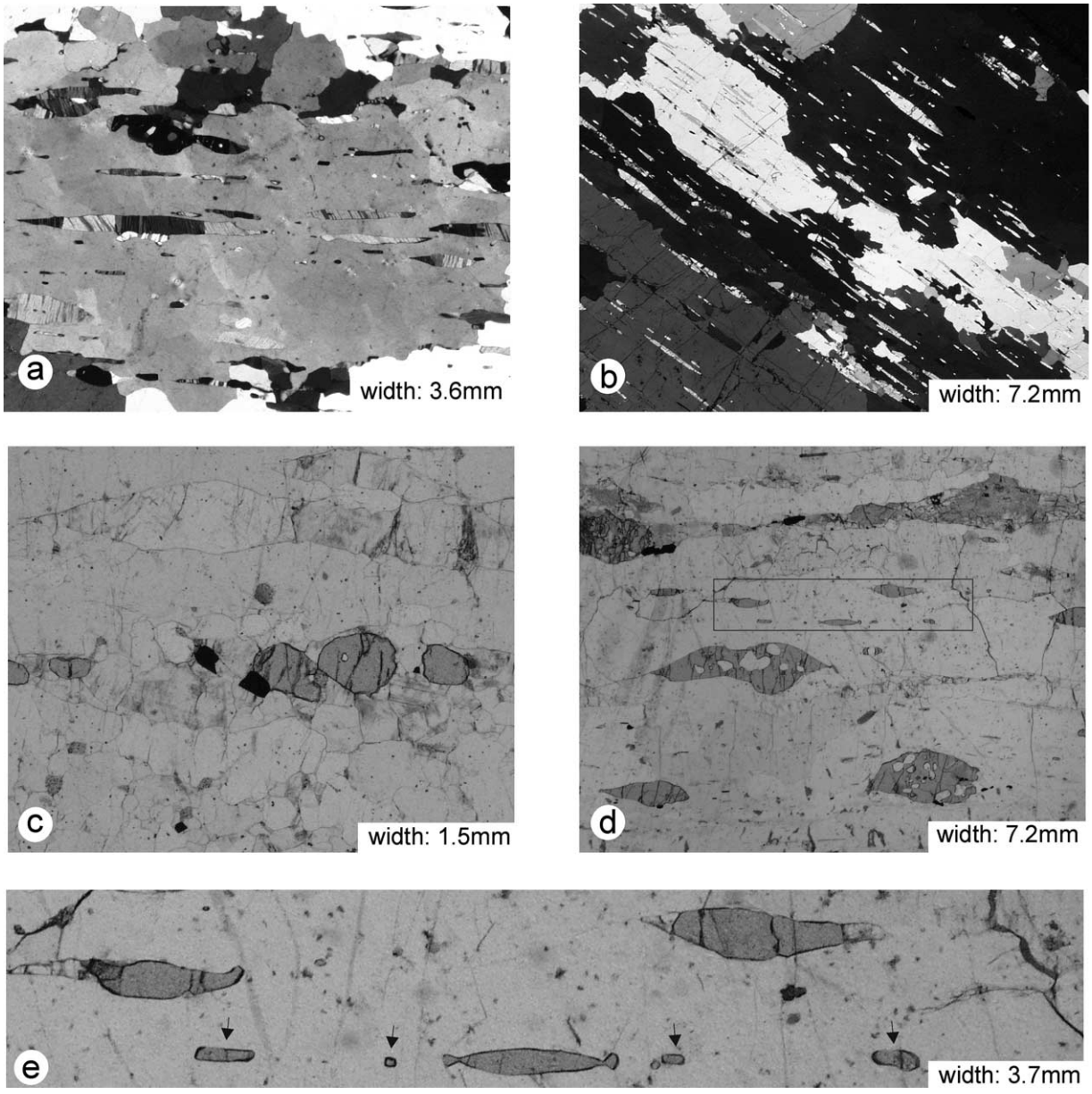

Fig. 3. Photomicrographs of fabrics in the planar deformed quartzites (L–S-fabric), all *XZ* sections. (a) Strings of KNa-feldspar, flame perthite formed after deformation. (b) Numerous sillimanites, perfectly oriented with *c*-axes in L1, included in large quartz grains with serrate grain boundaries. S1 parallel crystal faces often pinned to sillimanite. *X*-oriented diagonal (NW–SE). (c) Shear sliding of garnet fragments on fractures followed by drifting apart of the pieces. (d) Strongly elongate garnets. Frame marks position of (e). (e) Brittle–plastic behavior: small grains are pinched by the elongate grain and drift away (marked by arrows).

Fig. 4. Photomicrographs of fabrics in the folded quartzite (all *YZ*-sections). (a) Large quartz grain oriented with the long axis in the axial plane (S2, about vertical), grain boundary pinned by sillimanite grains. Sillimanites are cut normal to ⟨*c*⟩ and show preferred orientation of flat sides (010) in S2. (b) Buckled feldspar lens, with partial reorientation in S2. (c) Buckled garnet and feldspars and feldspar aggregates reoriented in S2. Especially small KNa-feldspars in quartz are well oriented with their long axes in S2. At the left margin a Fry-plot of distribution of secondary phases. (d) Blow up from (c): the feldspar aggregate is composed of polygonal plagioclase and sillimanite. Nearly no twins are visible, because the (010)-plane of feldspars has a preferred orientation in a high angle to *X*, i.e. they are close to the section plane. (e) Folded previously elongated garnet grain. (f) Folding of garnet with an initially less high aspect ratio.

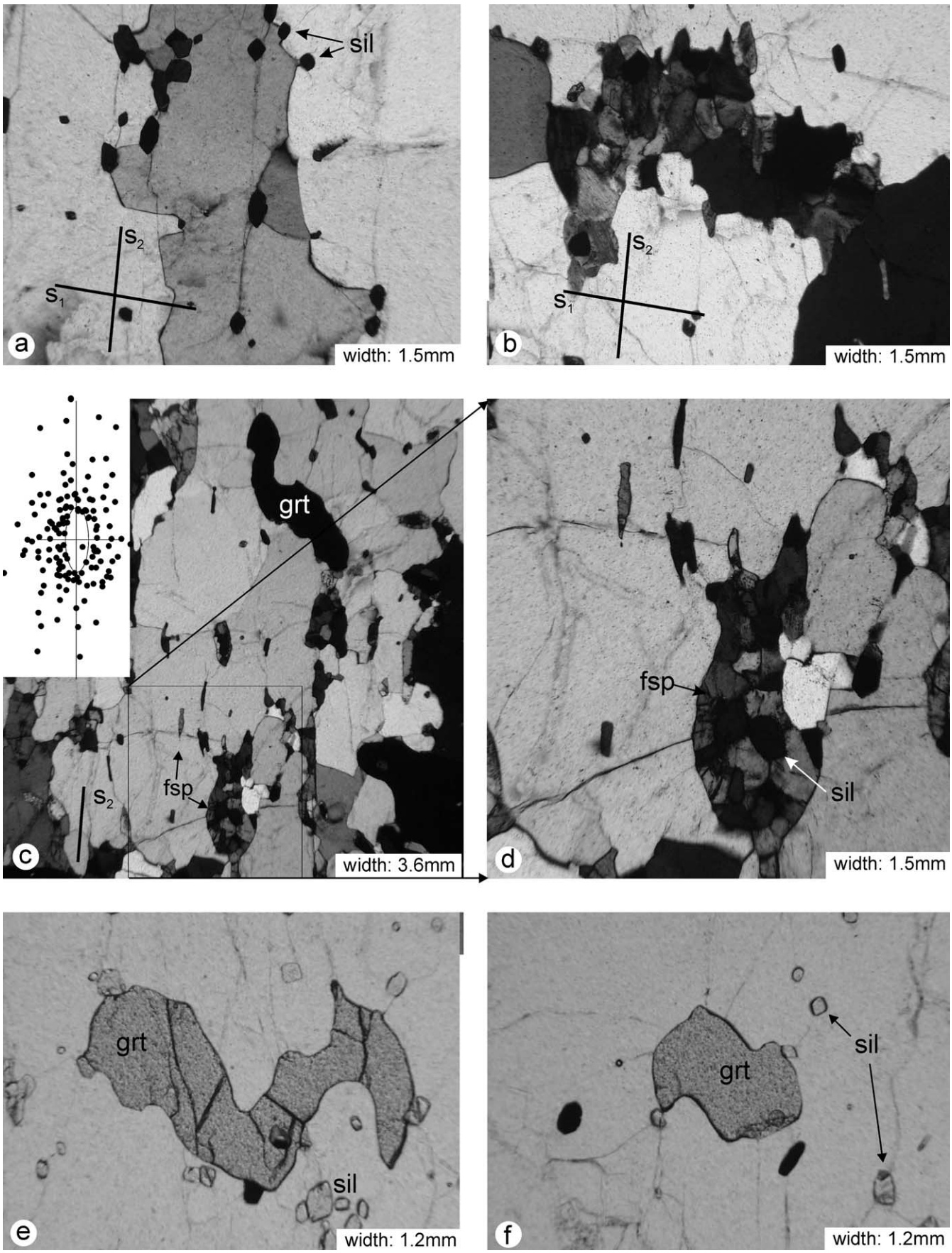
sil
s_2
s_1
a
width: 1.5mm
s_2
s_1
b
width: 1.5mm
grt
fsp
s_2
c
width: 3.6mm
fsp
sil
d
width: 1.5mm
grt
sil
e
width: 1.2mm
grt
sil
f
width: 1.2mm

3.2. The folded fabrics

Sections from the folded sample, cut parallel to the stretching lineation and normal to S1, show similar fabrics as described above for the planar *XZ* sections, both on the limbs and in the hinge of the fold. S1 in such sections is not as exactly straight as in *XZ* sections of the planar fabrics and the grain boundaries of the coarse quartz grains are less regular.

In sections normal to the stretching lineation/fold axes the fabric is quite different. The coarse quartz grains show similar irregular grain boundaries, commonly pinned by other phases such as sillimanite, but they have a crudely developed preferred orientation of their long axes parallel to the axial plane cleavage (Fig. 4a), in a high angle to S1, which mainly is defined by long axes of feldspar aggregates and sillimanite (010) planes (see below). The shape of the coarsened quartz grains is controlled by the distribution of other phases. Using the 'Fry-method' (Fry, 1979) on secondary phases in sections normal to the fold axes, an ellipse with the long axis strictly parallel to the axial plane and an axial ratio of about 1:2.2 can be derived (Fig. 4c; Fry diagram derived for a larger area than seen in the photograph). This value cannot be regarded as a measure of strain, as the distribution of secondary phases was not isotropic prior to folding, but it seems that the distribution of these phases reflects the flattening component normal to the axial plane.

Lensoidal feldspar aggregates are reoriented parallel to the new axial plane. Such lenses are formed by polygonal, recrystallized plagioclase and alkali–feldspar grains (Fig. 4b and c). Small individual alkali–feldspar grains included in quartz have a distinct elongate shape and are strictly aligned with their flat sides defining the new axial plane foliation (Fig. 4c and d).

Sillimanite displays rhomb-shaped or ellipsoidal cross-sections normal to *c* and a set of (010) cleavage planes. The sillimanite crystals are oriented with this plane sub-parallel to the axial plane.

Garnets, especially those with higher aspect ratios prior to the formation of the fold display a distinctly folded shape as shown in Fig. 4c, e and f. Such delicate structures of folded garnets have not been altered significantly by grain-boundary migration during high-*T* annealing. Often garnet–quartz phase boundaries show an acute dihedral angle at triple junctions, indicating that garnet–quartz phase boundaries have a lower interfacial energy than quartz–quartz grain boundaries. Nevertheless, similar to the planar fabrics the overall garnet shape is only slightly modified, no post-deformational spheroidization or other

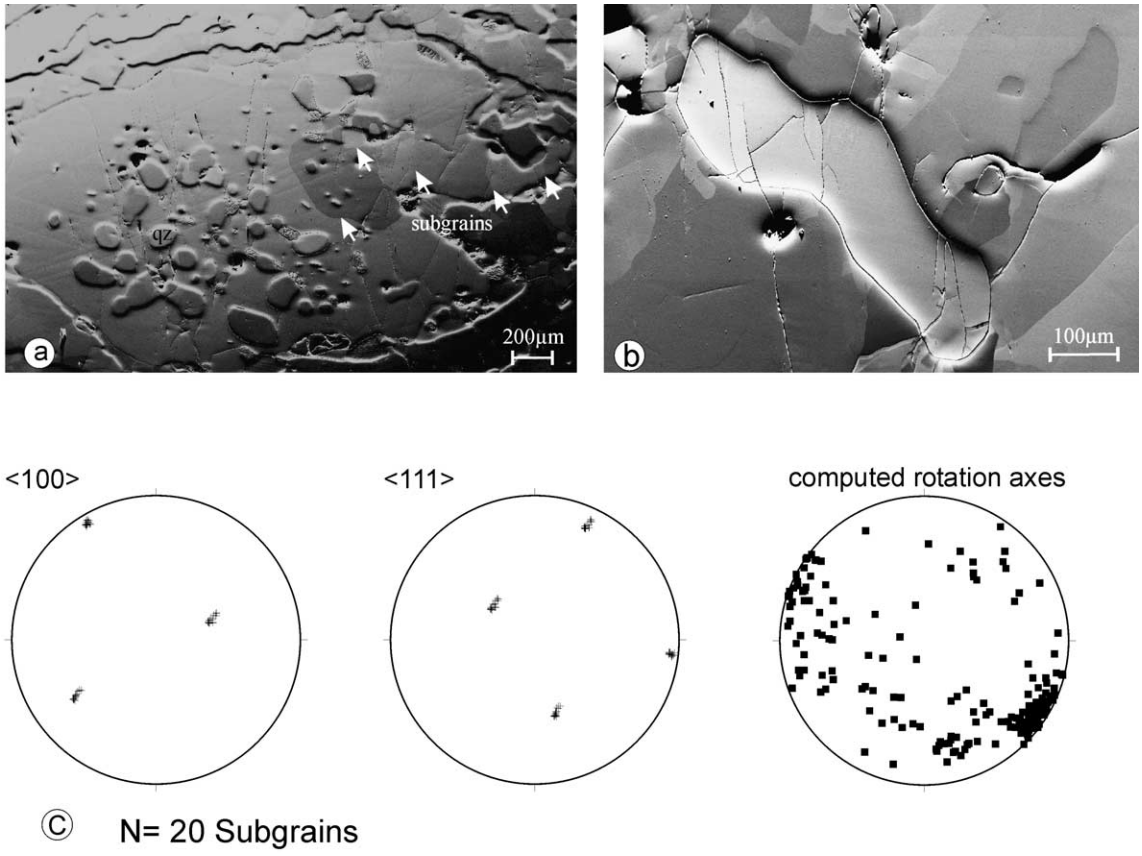

Fig. 5. OC-images of garnets. (a) Large garnet with some large subgrains. This is one of the garnets with the most subgrains found in these rocks. (b) A folded garnet, free of subgrains. (c) Orientation of ⟨100⟩ and ⟨111⟩ in the subgrains of (a) and calculated rotation axes between all subgrains. (Schmidt net, lower hemisphere).

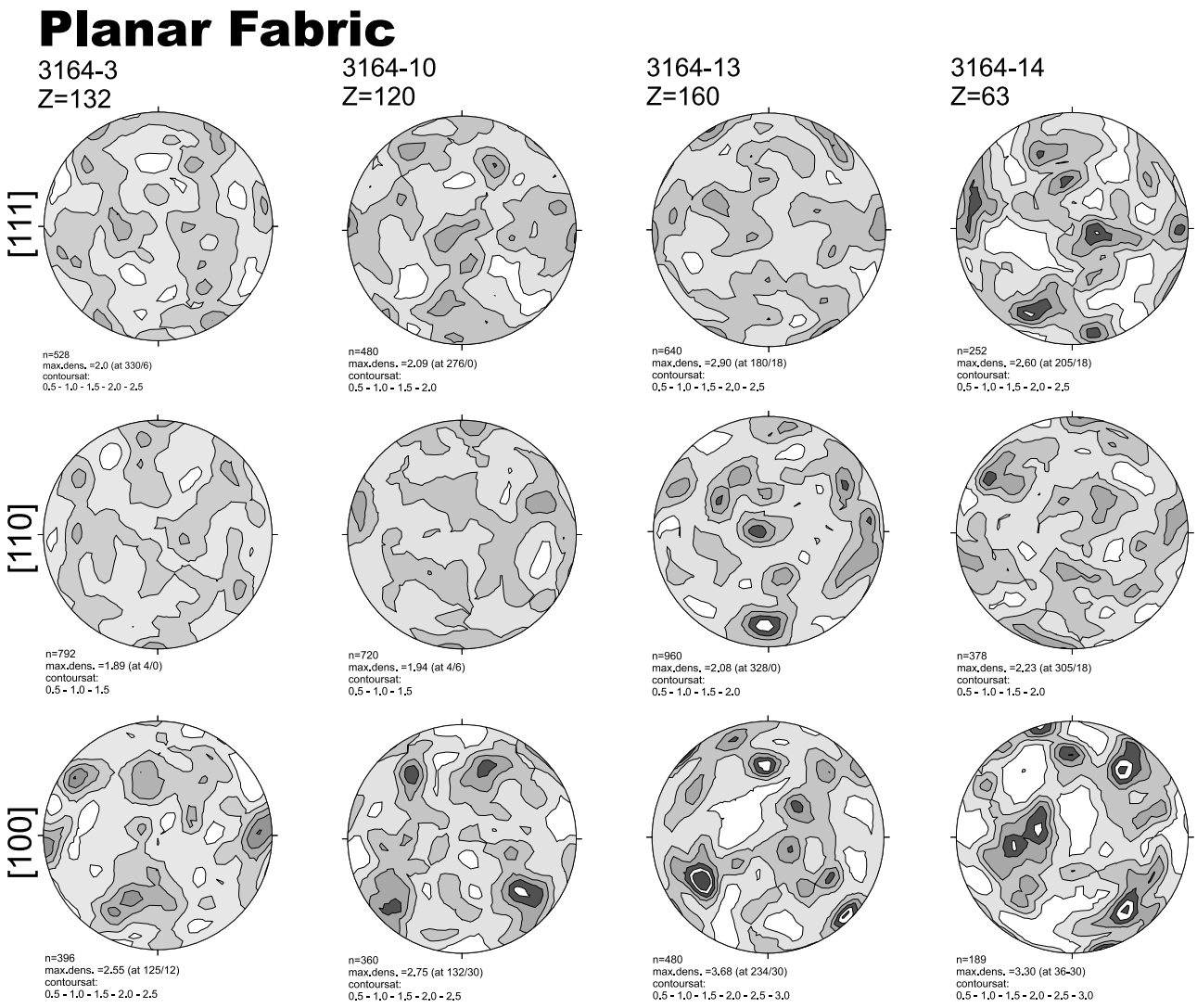

Fig. 6. Preferred orientation of garnet in thin sections from different domains (feldspar and sillimanite content, quartz grainsize) of sample 3164 (Z = number of grains; n = number of directions plotted) (contour levels are multiples of random distribution, Schmidt net, lower hemisphere).

processes to reduce grain boundary area of this peculiar shaped garnets can be found.

Summing up, the fabric is completely reoriented during folding. Quartz has coarsened post-deformational, but it reflects the reorientation parallel to the axial plane due to pinning of grain boundaries to minor phases. The resulting highly irregular shapes of garnet are well preserved.

4. Results from observations and measurements under the SEM

Thin sections of 30 μm thickness polished mechanically on both sides were prepared, subsequently polished chemically on one side using Syton on a micro-fiber cloth and coated with a thin layer of carbon.

EBSD patterns were generated using a field emission gun SEM LEO 1530 operated at 25 kV acceleration voltage and 25 mm working distance. The patterns were recorded from a scintillator screen by a camera from J. Jelen, indexing of the patterns was performed using the software Channel + from HKL Software, Hobro, Denmark.

Before measurements were taken, a map of each thin section was prepared from a transmitted light microscope image. Every garnet in the thin section was measured. The correct indexing of each grain was checked by comparing the generated Kikuchi lines with the simulation. Orientation contrast images were acquired using a quadrupol BSE detector mounted at a high angle to the electron beam.

4.1. OC-images

Significantly elongate garnets in the planar fabrics usually show few or commonly no subdomains in OC-images in our samples (cf. Kleinschrodt and McGrew, 1995, 2000). Only larger (several millimeter–centimeter),

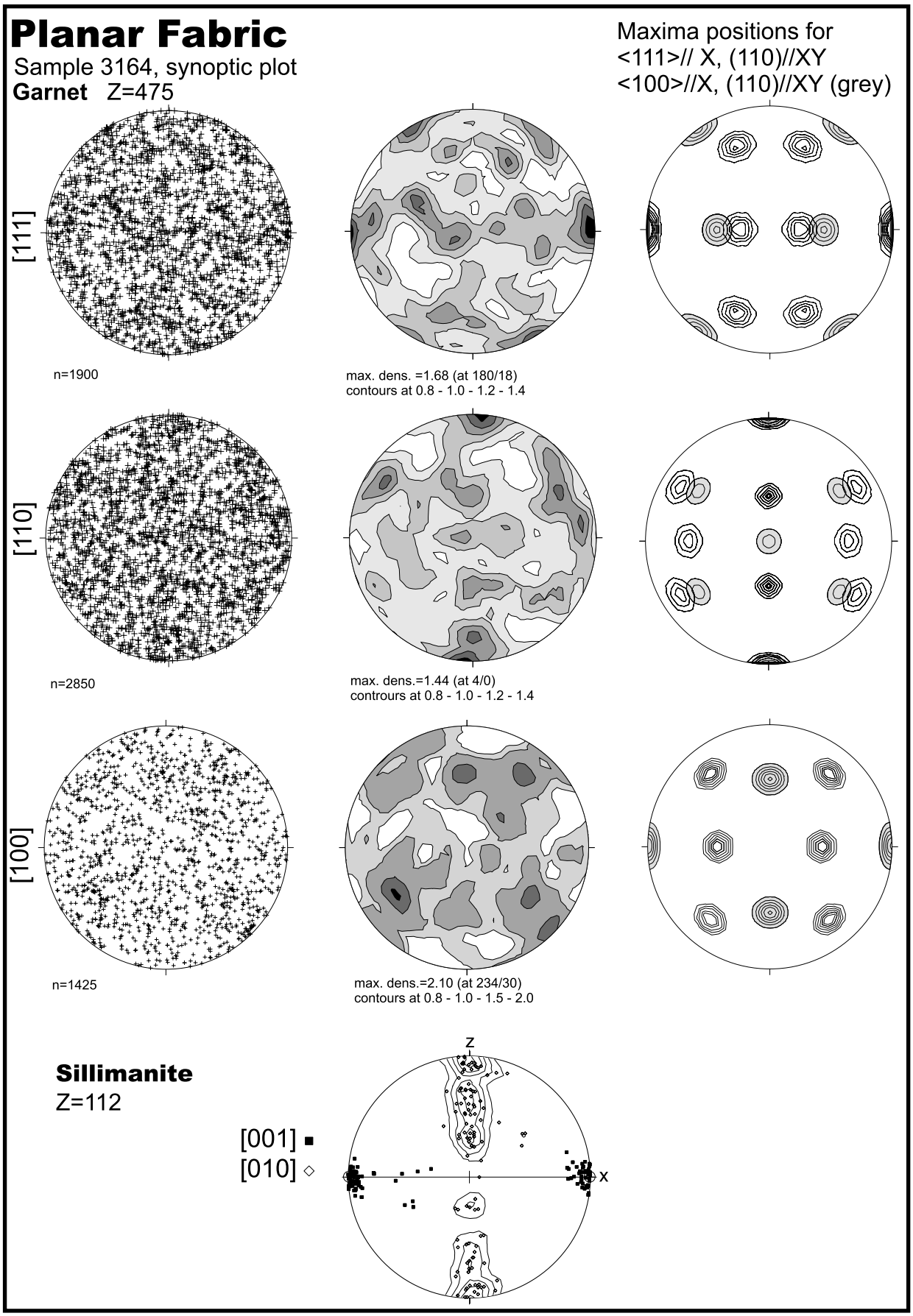
Planar Fabric
Sample 3164, synoptic plot
Garnet Z=475
Maxima positions for
<111>// X, (110)//XY
<100>//X, (110)//XY (grey)
[111]
n=1900
max. dens. =1.68 (at 180/18)
contours at 0.8 - 1.0 - 1.2 - 1.4
[110]
n=2850
max. dens.=1.44 (at 4/0)
contrours at 0.8 - 1.0 - 1.2 - 1.4
[100]
n=1425
max. dens.=2.10 (at 234/30)
contours at 0.8 - 1.0 - 1.5 - 2.0
Sillimanite
Z=112
[001] ■
[010] ◇
Z
X

inclusion-rich (quartz, sillimanite) garnets show a restricted number of subgrains (Fig. 5a). The subdomains often have curved boundaries, starting or ending at inclusions or at grain margins. The subdomain size is usually coarse, with an average diameter of several hundred microns. The misorientation across the subdomain walls is small (Fig. 5c). For such small misorientations the precision of a single measurement is not sufficient to derive rotation axis and slip system (Prior, 1999). Therefore calculated rotation axes show a vast spread of orientations, but significantly not a random pattern.

In the folded fabrics even garnets that are significantly folded usually show no subgrains (Fig. 5b). Sometimes one or two subdomains are found, usually at the ends of the crystals and the boundaries commonly are curved and connected to inclusions and grain margins.

4.2. Crystallographic preferred orientation

Textures were measured for garnet and sillimanite in the planar and folded fabrics. Orientations of *X*, *Y* and *Z* coordinate systems were fixed macroscopically. Sillimanite is regarded as an internal reference system to check that the samples are cut correctly. In general, ⟨001⟩ of sillimanite shows a preferred orientation parallel to the stretching lineation (*X*) and (010) a preferred orientation parallel to the flattening plane. In other words, (010) is oriented in the *XY* plane of the planar fabrics, and reoriented in the axial plane of the folded fabrics.

4.2.1. Planar fabrics

The textures of garnets are summarized in Figs. 6 and 7. The sillimanite texture displayed in the lower part of Fig. 7, with *c*-axes maximum in *X* and (010) maximum in *Z*, shows that the thin-sections are cut nearly perfectly in the *XZ*-plane. Garnets were measured in four domains from sample 3164, which were cut from garnet-bearing layers in the sample. The thin sections differ slightly in their content of secondary minerals, and therefore also quartz grain-size. Even though the textures of the individual thin sections are not identical, they show some common tendencies (Fig. 6):

1. ⟨111⟩ axes are arranged on a broad central girdle or on two separate small circle girdles normal or in a large angle to *X*. Close to *X* usually a maximum or at least a zone with higher *c*-axes concentration appears. In some diagrams a slight obliquity in relation to *X* is found, which is not the effect of an oblique section, as can be clearly seen in relation to the sillimanite (001) orientation in Fig. 7.
2. The (110) poles usually display one of the maxima normal to the foliation. The other poles are arranged on a central girdle normal to *X* and two small circle girdles in an angle of about 30° to *X*. Only 3164-3 shows a pair of maxima symmetrically disposed in an angle of 25° around *Z*.
3. The (100) poles are arranged on two small circle girdles in a moderate angle to *X*. In this respect 3164-3 forms an exception, as it shows a maximum in X, a feature not seen in any of the other diagrams.

A synoptic plot of all the data (Fig. 7) shows similar features like those described before and the exceptions described are smoothed out.

Interpretation of the textures: The pole positions of garnet oriented with a ⟨111⟩ direction in *X* and a {110} plane in *XY* (two different garnet orientations possible) are displayed in the diagrams in the right column of Fig. 7. Additionally a second orientation with ⟨100⟩ direction in *X* and also a {110} plane in *XY* is displayed (gray shaded). The general outline of the patterns and most of the ⟨111⟩ and {110} maxima coincide quite well with the first orientation and some of the additional maxima fit very well to the second. Although not every maximum is exactly matched, the overall distribution of the maxima, the symmetry of the pattern as a whole and the fit of several maxima in the synoptic (especially the pronounced ⟨111⟩ maximum in *X*) and the single plots strongly indicates the predominant activity of the 1/2⟨111⟩{110} slip system in garnet. There may be some contributions by slip systems with ⟨100⟩ Burgers vector. The maximum of [100] poles close to *X* in sample 3164-3 (Fig. 6) suggests that also ⟨100⟩ is a possible slip direction. ⟨100⟩(010) has also been described as possible slip system in garnet (Voegele et al., 1998). If this slip system would be active, an orientation of (010) parallel to the flow plane is to be expected. Yet, the (100) pole figure does not show a maximum normal to the foliation, but the other two corresponding maxima lie intermediate between *Y* and *Z*. Therefore a ⟨100⟩(010) slip system seems unrealistic. Slip with a ⟨100⟩ Burgers vector on a {110} plane is not a commonly assumed slip system in garnet, but some of the maxima visible in the ⟨111⟩ and {110} diagrams of sample 3164-3 (Fig. 6) could be much better explained by such a slip system (compare with gray shaded maxima in right row of Fig. 7). The marginal maxima of ⟨111⟩ on the girdles around *X* and also the (100) maxima between *Z* and *Y* are in accordance with an end orientation with ⟨100⟩ in *X* and a {110} plane close to the foliation. Such slip systems are common in f.c.c. metals.

It has been argued (e.g. Voegele et al., 1998) that 1/2⟨111⟩(110) is the slip system with the lowest activation

Fig. 7. Preferred orientations of all garnets in sample 3164 (planar fabric) (all *XZ*-sections, orientation like the sillimanite diagram): left row: point plot, central row: contoured pole diagram (contour levels are multiples of random distribution, Schmidt net, lower hemisphere). Right row: Schematic diagram of orientation of respective garnet axes with garnet oriented with one ⟨111⟩ direction in *X* and a (110) plane in *XY* and in gray with one ⟨100⟩ direction in *X* and a (110) plane in *XY*. In the lower part preferred orientation of sillimanite in the same sample.

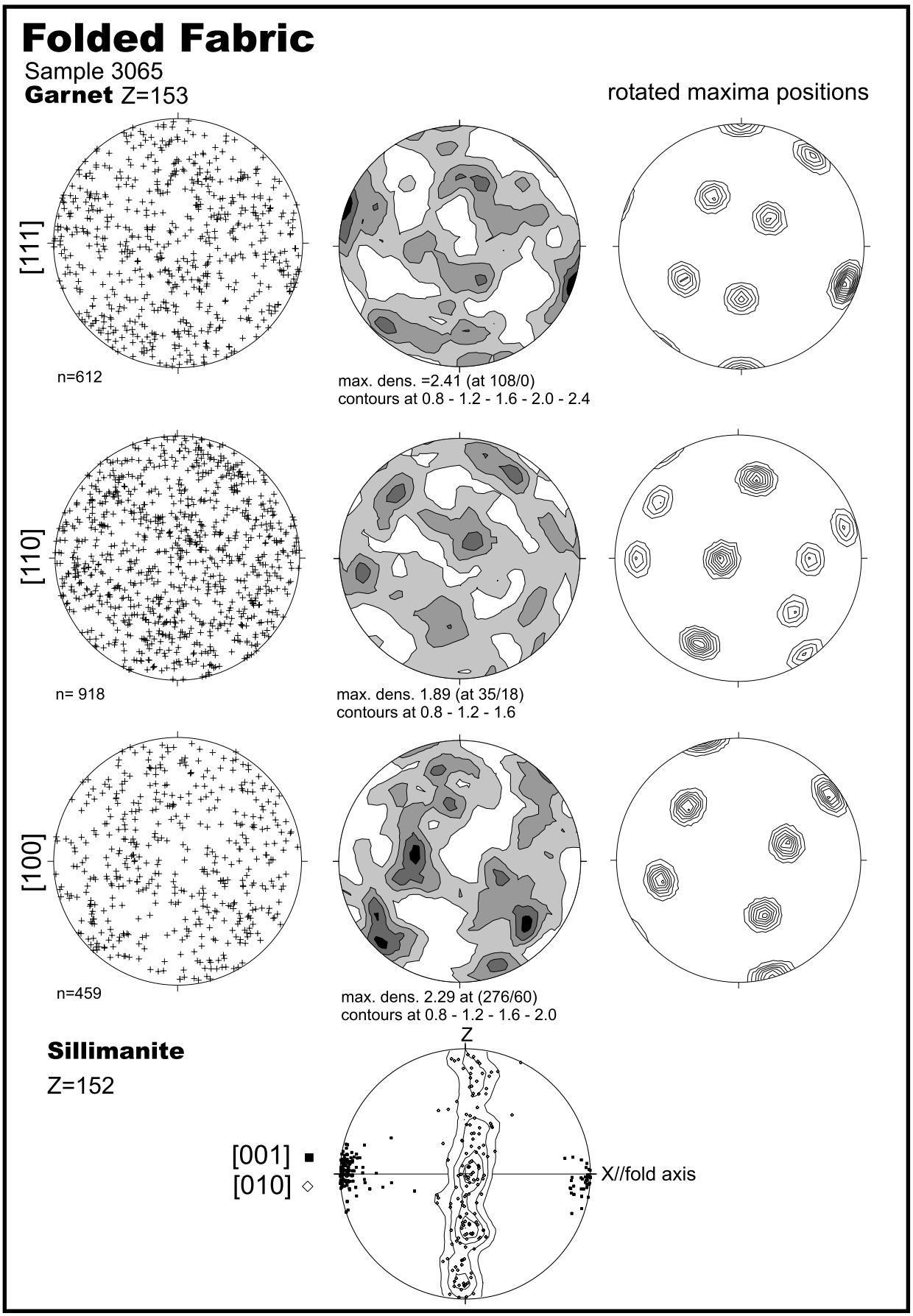
Folded Fabric
Sample 3065
Garnet Z=153
rotated maxima positions
[111]
n=612
max. dens. =2.41 (at 108/0)
contours at 0.8 - 1.2 - 1.6 - 2.0 - 2.4
[110]
n= 918
max. dens. 1.89 (at 35/18)
contours at 0.8 - 1.2 - 1.6
[100]
n=459
max. dens. 2.29 at (276/60)
contours at 0.8 - 1.2 - 1.6 - 2.0
Sillimanite
Z=152
Z
[001] ■
[010] ◇
X//fold axis

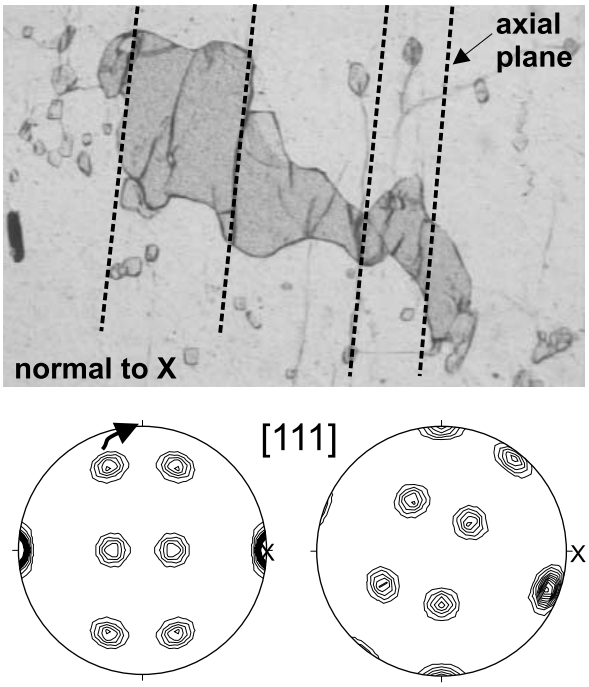

Fig. 9. Folded garnet with schematic axial plane parallel slip planes. Rotation of one ⟨111⟩ axis form the theoretical initial planar fabric into parallelism with the indicated shear planes (= axial plane) and normal to the fold axis.

stress and that it is the one predominant in nature (Wang and Ji, 1999). Most features of the textures can be explained by such a mechanism, but an additional contribution of ⟨100⟩ slip on {011} would explain some of the observed maxima.

The low intensities have the consequence that the resulting patterns are sensible with respect to contouring modes. Testing our patterns with different contouring modes using the program 'StereoNett' by J. Duyster (available from his website at http://homepage.ruhr-uni-bochum.de/Johannes.P.Duyster/) the general pattern and the most pronounced maxima remain unchanged, only weaker (sub-) maxima may form or disappear. In general, in textures of cubic minerals with their multiple symmetrically equivalent slip systems the arrangement of areas with intensities above average distribution (i.e. the 'skeleton' as used for interpretation of quartz *c*-axes fabrics) is more important than the position of an individual maximum.

4.2.2. Folded fabrics

Textures of garnet and sillimanite are displayed in Fig. 8 with the fold axis/stretching lineation in the horizontal diameter and the axial plane parallel to the projection plane of the diagram (for a better comparison with the planar fabrics, the direction in the axial plane and normal to the fold axis is labelled *Z*, which is the rotated *Z* from D1). The sillimanite still shows a pronounced maximum of ⟨001⟩ parallel to the stretching lineation. The fold axis therefore is exactly parallel to the stretching lineation, otherwise a small circle distribution of the sillimanite *c*-axes around the fold axis would be expected. The (010) poles are distributed on a girdle normal to the stretching lineation, a maximum is developed normal to the axial plane, i.e. numerous sillimanites are oriented with (010) in the axial plane of the fold. The sillimanites can again be used as an internal reference system in relation to folding, defining the fold axis and the axial plane very well. The axial plane is otherwise not visible, as a clearly defined plane (like for example marked by micas in mica schists) is missing.

The garnets show a ⟨111⟩ maximum close to the stretching lineation, but with a distinct obliquity of about 15° (stretching lineation parallel to fold axis and marked by sillimanite ⟨*c*⟩-axes). The other maxima are mainly arranged on or close to the *YZ* plane. The {110} planes show one maximum about normal to the axial plane. The other (110) maxima seem to be aligned on oblique (in relation to *XYZ*) small circles. The (100) poles form maxima on two small circle girdles, again slightly oblique to the *XYZ* reference system.

Interpretation of textures: If one assumes the folded rock previously had a texture similar to the planar fabric (and the folded sample must have gone through this stage), the following modifications of the texture seem to be most important. The clear and symmetric texture of ⟨111⟩ axes is lost. Significantly, the ⟨111⟩-maximum close to the stretching lineation is offset from the stretching lineation. This is clearly not a cutting effect, as shown by the sillimanite reference system. The other maxima are located on two small circle girdles in a large angle to the maximum oblique to *X*. We assume that folding of garnets is not accomplished by flexure of their lattice but by a shear-fold type mechanism, where a slip plane and direction rotate into the axial plane and the direction normal to the fold axis (Fig. 9). The dominant slip system in garnet reorients in this new reference frame: one ⟨111⟩ position close to *Z* from the theoretical ⟨111⟩ diagram of Fig. 7 was chosen and rotated towards *Z*. The diagrams for {110} and {100} were rotated in the same way and all are displayed in the right column of Fig. 8. In the ⟨111⟩ diagram it now is clear that the marginal maximum oblique to *X* is a geometrical consequence of the ⟨111⟩ rotation towards *Z*, not due to a rotational (or simple shear) component parallel to *X*. The general pattern shows quite good correlation to the theoretical one. An even better correlation can be seen comparing the {110} patterns. One effect of the small rotation is also that one {110} pole rotates automatically towards a position close to *Y*, i.e. with the

Fig. 8. Preferred orientations of garnets in sample 3065 (folded fabric) (all *XZ*-sections, *X* on the horizontal diameter, for better comparison *Z* is taken from D1, i.e. the projection plane is parallel to the axial plane): left row: point plot (Schmidt net, lower hemisphere), central row: contoured pole diagram (contour levels are multiples of random distribution). Right row: rotated schematic diagram of Fig. 7, rotation according to Fig. 9. This rotation was applied to all schematic diagrams. In the lower part preferred orientation of sillimanite in the same sample.

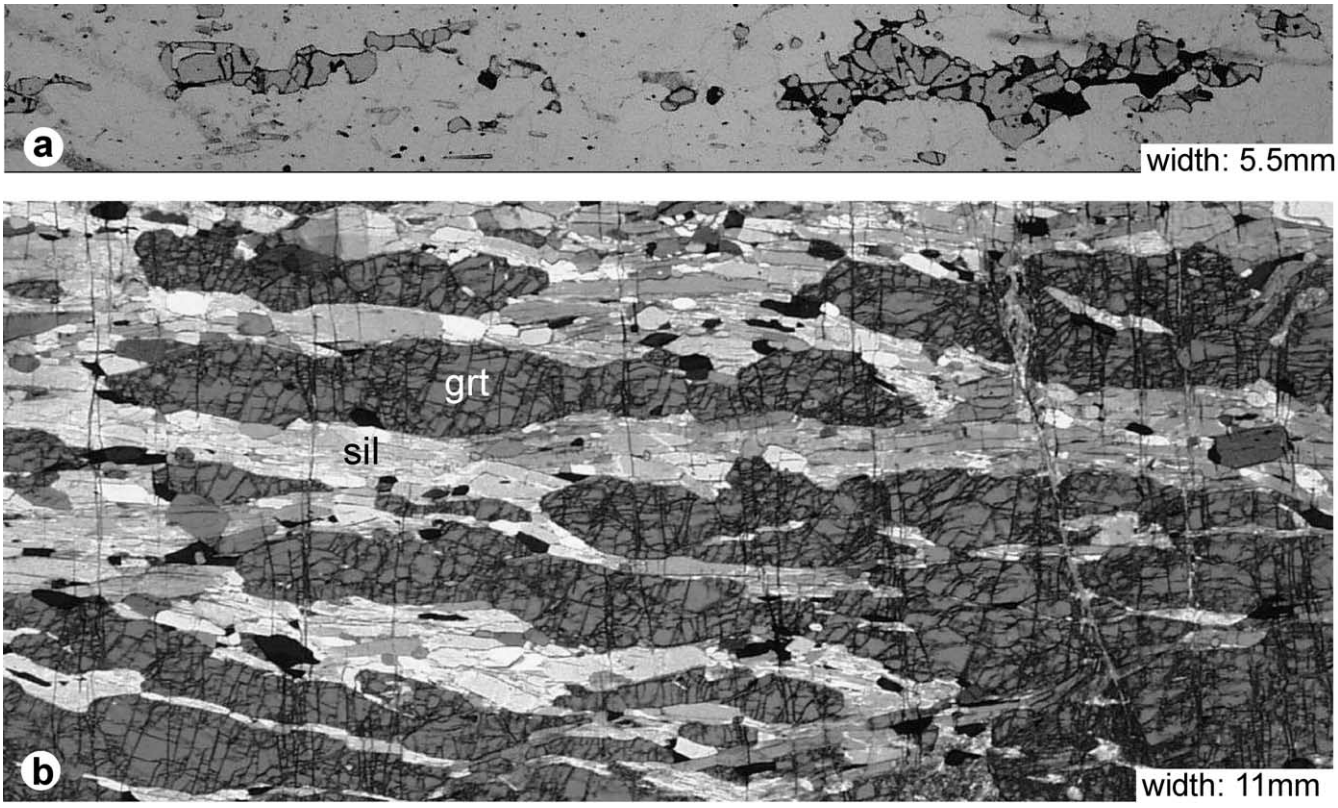

Fig. 10. Garnet microfabrics in samples (*XZ*-sections) from the Eastern Ghats and the Ivrea Zone. (a) Part of a garnet domain within the sample from the Eastern Ghats. Separate elongate grains and fragmentation of larger garnet pieces. Plane polarized light.(b) Elongate garnets embedded in a sillimanite matrix from the Ivrea Zone. Polarizers obliquely crossed.

supposed slip plane towards the axial plane. The general {100} pattern again correlates well with the theoretical one. There is no indication that in this case also an ⟨100⟩ slip direction contributes to the pattern.

It is astonishing that the simple rotation of one ⟨111⟩ axis into the axial plane and normal to the fold axis can explain most of the observed features in the folded fabrics. Combining the maxima of the rotation of both ⟨111⟩ maxima close to *Z* (upper two maxima in the theoretical ⟨111⟩ plot in Fig. 7) towards *Z* a pattern distinctly different form the measured ones results and especially the oblique ⟨111⟩ maximum close to *X* is replaced by maxima symmetrically distributed around *X*. Therefore, during evolution of the natural pattern, one of these ⟨111⟩ positions is preferred. The fold axis is parallel to the stretching lineation, which may be associated with a simple shear component, but usually shear indicators are absent and the microstructures are highly symmetrical. If such a component is active during formation of the fold, than one could imagine that a ⟨111⟩ position, which rotates with the bulk rotation would be preferred.

5. Examples from the Eastern Ghats/India and the Ivrea Zone/N-Italy

In spite of the increased interest in the deformational behavior of garnets, which is essentially triggered by the availability of the ECP and EBSD techniques, up to now no garnet textures from other granulite terrains than Sri Lanka and the Grenville are available. Two examples from the granulite terrains of the Eastern Ghats/India and the Ivrea Zone/Italy were chosen for a comparison with the samples from Sri Lanka.

The sample from the Eastern Ghats is a garnet-bearing quartzite from the country rocks of the Bolangir anorthosite (about 1 km west of the contact). The rock is very similar to the Sri Lankan rocks, with clear foliation and stretching lineation. Deformation in the contact zone occurred at *T* of about 800–750 °C (Raith et al., 1997). Like in the Sri Lankan sample the garnets have an almandine-rich composition and show similar deformation features, especially typical dumb-bell shapes. One difference is that the garnets occur in domains of numerous garnets aligned parallel to the foliation, strongly suggesting that each domain is derived from a single large garnet fragmented into numerous small grains (Fig. 10a) deformed within a ductilely flowing quartz matrix. Such domains are better preserved, than in comparable Sri Lankan samples. It is suspected that in the later case the domainal arrangement has been lost due to much stronger matrix deformation (i.e. the garnet fragments have drifted apart so far that they can no longer be recognized as a part of a former domain). OC-images

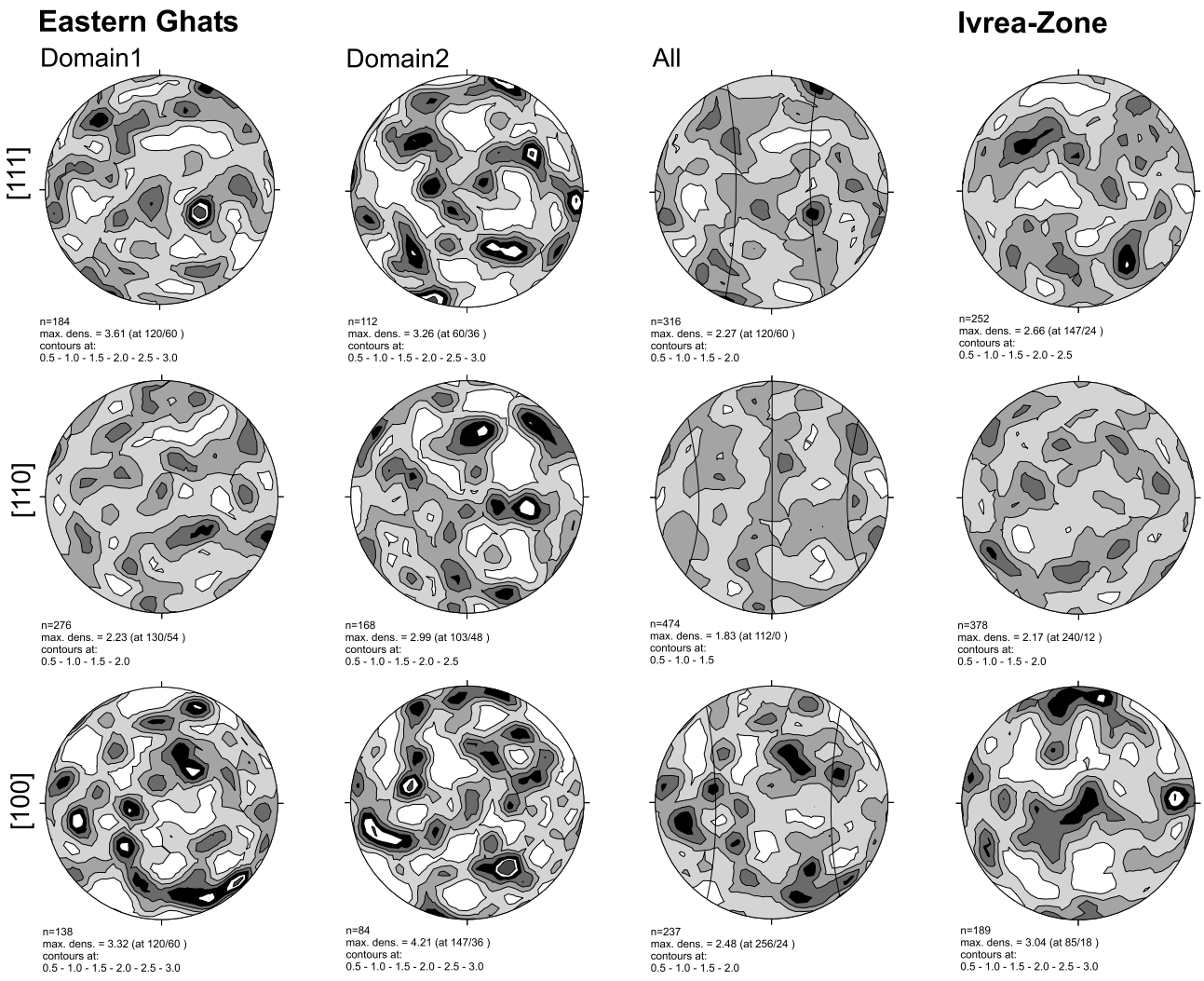

Fig. 11. Preferred orientations of garnets in samples from the Eastern Ghats and the Ivrea Zone (all *XZ*-sections, *X* on the horizontal diameter, contour levels are multiples of random distribution, Schmidt net, lower hemisphere). Three columns to the left are from the Eastern Ghats sample (two different elongate garnet domains with 46 and 28 garnets and a synoptic plot). The small circles on which maxima for ⟨111⟩ slip direction and (110) slip plane would plot (compare theoretical diagrams in Fig. 7) are indicated. Right column shows preferred orientation in a sample from the Ivrea Zone. Note the {100} maxima close to *X*, *Y* and *Z*.

show that the garnets again are nearly free of subgrains. In two domains all grains were measured. The patterns derived for each domain are different in relation to the positions of individual maxima (Fig. 11). For example, the position of the largest maximum of (110) poles in Domain 2 is nearly a minimum in Domain 1 and the single domain diagrams are hard to explain. However, the synoptic plot again shows a pattern similar to the Sri Lankan one, with one of the ⟨111⟩ maxima close to *X* and the others arranged on small circle girdles, and a maximum of (110) poles close to *Z*. For a better comparison, the skeleton of this end-orientation is outlined in the synoptic diagram of Fig. 11. The arrangement of maxima is in accordance with dominant 1/2⟨111⟩(110) slip. The difference of the domains shows that there is probably an influence of the initial lattice orientation of the parent garnet. The maximum of (100) in the vicinity to *X* may again indicate subordinate activity of slip systems with [100] Burgers vector.

The sample from the Ivrea Zone is a restitic granulite composed mainly of garnet and sillimanite from the deep part of the Val Strona cross-section (about 1.4 km west of Forno) with a well defined LS-fabric. Peak temperatures derived from garnet–clinopyroxene thermometry in neighboring rocks yield 730 ± 30 °C, in accordance with data published by Henk et al. (1997) for this area. Garnets in this sample are up to several millimeters in dimensions with aspect ratios up to 4.5 in *XZ* sections (Fig. 10b). The garnet composition (alm56 prp40 grs3) is distinctly different from the examples from Sri Lanka and India. OC-images show some, generally large, subgrains with low misorientation angles (<4°). The preferred orientation patterns measured in this sample are well-defined and entirely different from the previous ones (Fig. 11). The {100}

poles form three maxima close to the *X*-, *Y*- and *Z*-axes. The (110) pole maxima are situated diagonal between *XY*, *YZ* and *XZ*, and the ⟨111⟩ poles diagonal between *XYZ*. This agrees exactly with an end orientation derived for a dominant [100](010) slip system, which has been reported to be the most probable one besides 1/2⟨111⟩(110) based on TEM analyses of experimentally and naturally deformed garnets (Karato et al., 1995; Voegele et al., 1998). No other texture components that would argue for additional slip systems are present.

6. Discussion

Pressure solution and preferred growth of garnets have been proposed as mechanisms producing elongate garnets, but both mechanisms cannot produce the garnet structures described from the fold hinge. The only mechanism that theoretically could explain the shape of the folded garnets could be a kink-type folding/fracturing of the elongate garnets followed by healing of the fractures. Then one should expect different orientations in different parts of the folded garnets, but as the orientation contrast images demonstrate, this can definitely be ruled out for many of the folded garnets. They frequently are single crystals with few or no substructures. Few separate garnets in contact with each other with different crystallographic orientation can be found in the folded sample and are explained as initially two different garnets having approached each other during folding and associated shortening. These garnets demonstrate that if differently oriented garnets are in contact at high-angle grain boundaries, as it would be expected at a kink-plane, such boundaries are preserved and they can be detected by OC-imaging, but this is not the case for most of the garnets.

As the folded garnets form under similar high-temperature conditions (or even lower *T*) as the planar ones, this demonstrates for both cases that garnets can be plastically deformed.

6.1. Which deformation mechanisms are related to plastic deformation?

As intracrystalline microstructures can be erased by annealing or slow cooling from high temperatures and later stresses can introduce microstructures not related to the high-*T* deformation, textures may provide the only preserved information about deformation mechanisms under peak conditions. The preferred orientation patterns of garnet from Sri Lanka and India indicate that dislocation glide with 1/2⟨111⟩{110} slip system is the dominant deformation mechanism, with some contributions of a slip system with [100] Burgers vector.

The observation that there is a grain size dependence of the deformation (high elongation and deformation microstructures were only found in small garnets) is interpreted to indicate that diffusion controlled processes may interact with dislocation creep (Kleinschrodt and McGrew, 1995, 2000). Smaller garnets probably result from the fracturing of larger grains and drifting apart of the fragments. Therefore, smaller garnets also differ in shape prior to plastical deformation from the larger ones (tabular slices the first, more spherical the latter), which makes a correlation between grainsize and aspect ratio rather difficult. The interaction of brittle and plastical deformation documented by the boudinaged and finally fractured grains (Fig. 3e) supports the interpretation of Wang and Ji (1999), that almandine rich garnets at temperatures of 750–850 °C and strain rates of 10^{-14} to 10^{-15} are in their brittle–ductile transition zone.

If subgrains formed during plastic deformation they are either healed out due to high temperatures after the end of deformation or the subgrain size is so coarse that no or only few can be found in the usually small elongate garnets. The few, large subgrains frequently have curved boundaries, different from the straight subgrain boundaries described by Prior et al. (1999, 2000). Small subgrains with more straight boundaries are uncommon, only few were preserved in hinges of folded garnet.

6.2. How reliable are the textures?

It has been argued that it is not expected that garnets deforming by a dislocation glide/creep mechanism will show distinct preferred orientations as numerous symmetrically equivalent slip planes and directions for each slip system will cause no significant rotation of lattice planes with respect to the strain axes (Ji and Martignole, 1996). Even though the textures described above demonstrate that distinct patterns form, this argumentation is supported by the low intensities of the maxima. In spite of the low intensities of the preferred orientations the general patterns and the arrangement of maxima can be related to ‘easy slip’ positions in the finite strain reference frame. Compared with minerals with only one dominant slip system like quartz at low temperatures, lattice rotations during deformation are small, as one of the equivalent slip systems is always close to a favorable position for slip. This is especially documented by the texture of the folded garnets, which can be very well explained by such a rotation to an ‘easy slip’-position.

The low intensities of the preferred orientations have a further consequence if we look for garnet textures in different rock types. In the examples from Sri Lanka and India presented in this study, the garnets are embedded in a homogeneously deforming matrix of quartz and the deformation is relatively simple with a clear strain reference frame from outcrop to microscope scale and a homogeneous stress field. Also, in the sample from the Ivrea Zone garnet deformation is homogeneous at least on the hand-specimen scale. As soon as the strain reference system is slightly disturbed on the grain scale, for example by interfering neighboring garnets (like for example commonly observed

in eclogites) or interference with other clasts disturbing the local stress field, it is to be expected that the texture patterns will be too weak, even if the garnets deform by dislocation glide/creep processes.

The example from Eastern Ghats/India may provide an explanation for slightly different patterns in different parts of a rock. As the plastic strain in single small garnet grains is probably not very high, there could be an influence of the parental garnet orientation for different domains. As the larger garnets are commonly fractured on a set of parallel planes, sliding on these fractures will not erase a preferred orientation, which could cause the observed differences between domains and also weaken the overall texture.

The occurrence of [100] maxima in *X* in sample 3164-3, and especially in the sample from the Ivrea Zone, documents that slip systems with a [100] Burgers vector may also be active, or as in the case of the Ivrea Zone sample, even be dominant. Based on textures {110} slip planes in the Sri Lankan sample and {010} in the Ivrea Zone sample can be derived. At the moment there is no clear explanation why the sample from the Ivrea Zone, deformed at only slightly lower temperatures, shows this different texture.

7. Conclusions

Garnets from Sri Lanka, first stretched and flattened, then subsequently folded allow the shedding of light on several controversial points regarding deformation of garnets:

1. Almandine-rich garnets are plastically deformed at 800 ± 50 °C and the deformed shapes are well preserved. Flow strength of garnet is low enough that it is deformed in a quartz matrix. In spite of slow cooling and initially high temperatures no grain-shape equilibration (grain surface reduction) of elongate or folded garnet occurred in the quartz matrix probably due to a low quartz/garnet phase boundary energy.
2. The scarcity of intracrystalline deformation substructures (subgrains) in garnet and frequently also in quartz argue for low stresses during the cooling/exhumation history of the terrain.
3. Garnet develops lattice preferred orientations under moderate strain and is readily reoriented as only small rotations are necessary that one of the equivalent slip planes and directions are in a favorable position. The intensity of preferred orientation is low but the general patterns are distinct and can be interpreted by 'easy slip' orientations of the dominant slip system.
4. 1/2⟨111⟩{110} is the dominant slip system in the Sri Lankan and Indian samples. Contributions by slip systems with a ⟨100⟩ Burgers vector and (110) slip plane can be derived from some textures. The texture from the Ivrea Zone sample indicates a dominant [100](010) slip system. This shows that other factors than temperature may control the dominant slip system.
5. Diffusion creep may interact with dislocation creep, but it is not clear to what extent.

The above observations show that garnet textures may provide important information about the deformational behavior of garnet in crustal rocks. The variable textures together with substructures that may be preserved or erased are a potential monitor of deformation conditions in the high temperature field. Still our knowledge on garnet plasticity is restricted and pending questions are: What is the lower temperature range of garnet plasticity? Under what conditions do subgrains form, and how are they erased? Does garnet show recrystallization under specific conditions? What controls the type of texture evolving? To what amount does diffusion creep contribute? Especially important will be future investigations in H*T*-eclogites and mantle rocks, where the behavior of garnet may be even more important for the whole rock rheology.

Acknowledgements

Financial support for parts of this study from the German Science Foundation within the scope of the Collaborative Research Center (SFB 526) "Rheology of the Earth—from the upper crust into the subduction zone" is gratefully acknowledged by J.D. Thanks to C. Dobmeier for providing the garnet–quartzite sample from the Eastern Ghats and to D. Prior for some OC-images and discussion at the beginning of the work. Critical reviews by J. Martignole and J. Kruhl and comments by G. Suhr on the early manuscript helped to improve the clarity of the text.

References

Blackburn, W.H., Dennen, W.H., 1968. Flattened garnets in strongly foliated gneisses from the Grenville Series of the Gananoque area, Ontario. American Mineralogist 53, 1386–1393.

den Brok, B., Kruhl, J., 1996. Ductility of garnet as an indicator of extremely high temperature deformation: discussion. Journal of Structural Geology 18, 1369–1373.

Dalziel, I.W., Bailey, S.W., 1968. Deformed garnets in a mylonitic rock from the Grenville front and their tectonic significance. American Journal of Science 266, 542–562.

Fry, N., 1979. Random point distributions and strain measurement in rocks. Tectonophysics 60, 89–105.

Ji, S., Martignole, J., 1994. Ductility of garnet as an indicator of extremely high temperature deformation. Journal of Structural Geology 16, 985–996.

Ji, S., Martignole, J., 1996. Ductility of garnet as an indicator of extremely high temperature deformation: Reply. Journal of Structural Geology 18, 1375–1379.

Henk, A., Franz, L., Teufel, S., Oncken, O., 1997. Magmatic underplating, extension and crustal reequilibration: Insights from a cross-section through the Ivrea Zone and Strona–Ceneri Zone, northern Italy. Journal of Geology 105, 367–377.

Karato, S., Wang, Z., Liu, B., Fujino, K., 1995. Plastic deformation of garnets: systematics and implications for the rheology of the mantle transition zone. Earth and Planetary Science Letters 130, 13–30.

Kleinschrodt, R., Voll, G., 1994. Deformation and metamorphic evolution

of a large-scale fold in the lower crust: the Dumbara synform, Sri Lanka. Journal of Structural Geology 16, 1495–1507.

Kleinschrodt, R., McGrew, A.J., 1995. Garnet plasticity in the lower continental crust: constraints on deformation mechanisms from microstructural and textural data. Journal Czech Geological Society 40/3, C-104.

Kleinschrodt, R., McGrew, A.J., 2000. Garnet plasticity in the lower continental crust: implications for deformation mechanisms based on microstructures and SEM electron channeling pattern analysis. Journal of Structural Geology 22, 795–809.

Lloyd, G.E., 1987. Atomic number and crystallographic contrast images with the SEM: a review of backscattered techniques. Mineralogical Magazine 51, 3–19.

Lloyd, G.E., 1994. An appreciation of the SEM electron channeling technique for petrofabric and microstructural analysis of geological material. In: Bunge, H.J., Siegesmund, S., Skrotzki, W., Weber, K. (Eds.). Textures of Geological Materials. DGM-Informationsgesellschaft, pp. 109–126.

Prior, D.J., 1999. Problems in determining the orientations of crystal misorientation axes for small angular misorientations, using electron backscatter diffraction in the SEM. Journal of Microscopy 195, 217–225.

Prior, D.J., Trimby, P.W., Weber, U.D., Dingely, D.J., 1996. Orientation contrast imaging of microstructures in rocks using forescatter detectors in the scanning electron microscope. Mineralogical Magazine 60, 859–869.

Prior, D.J., Boyle, A.B., Brenker, F., Cheadle, M.C., Day, A., Lopez, G., Peruzzo, L., Potts, G.J., Reddy, S., Spiess, R., Timms, N.E., Trimby, P., Wheeler, J., Zetterström, L., 1999. The application of electron backscatter diffraction and orientation contrast imaging in the SEM to textural problems in rocks. American Mineralogist 84, 1741–1759.

Prior, D.J., Wheeler, J., Brenker, F.E., Harte, B., Matthews, M., 2000. Crystal plasticity of natural garnet: new microstructural evidence. Geology 28, 1003–1006.

Raith, M., Bhattacharya, A., Hoernes, S., 1997. A HFSE- and REE-enriched ferrodiorite suite from the Bolangir anorthosite complex, Eastern Ghats Belt, India. Proceedings of the Indian Academy of Science (Earth and Planetary Sciences) 106, 299–311.

Voegele, V., Ando, J.I., Cordier, P., Liebermann, R.C., 1998. Plastic deformation of silicate garnet. I. High-pressure experiments. Physics of the Earth and Planetary Interiors 108, 305–318.

Voll, G., Evangelakakis, C., Kroll, H., 1994. Revised two-feldspar geothermometry applied to Sri Lankan feldspars. Precambrian Research 66, 351–378.

Wang, Z., Ji, S., 1999. Deformation of silicate garnets: Brittle ductile transition and its geological implications. The Canadian Mineralogist 37, 525–541.